Supporting Information

Non-halogenated Surface-Active Ionic Liquid as Electrolyte for Supercapacitors

Preeti Jain,*[a] Oleg N. Antzutkin[ab]

[a]*Chemistry of Interfaces, Luleå University of Technology, SE-97 187, Luleå, Sweden*
[b]*Department of Physics, Warwick University, CV4 7AL, Covertly, United Kingdom*

*E-mails: Preeti.Jain@ltu.se; Oleg.Antzutkin@ltu.se

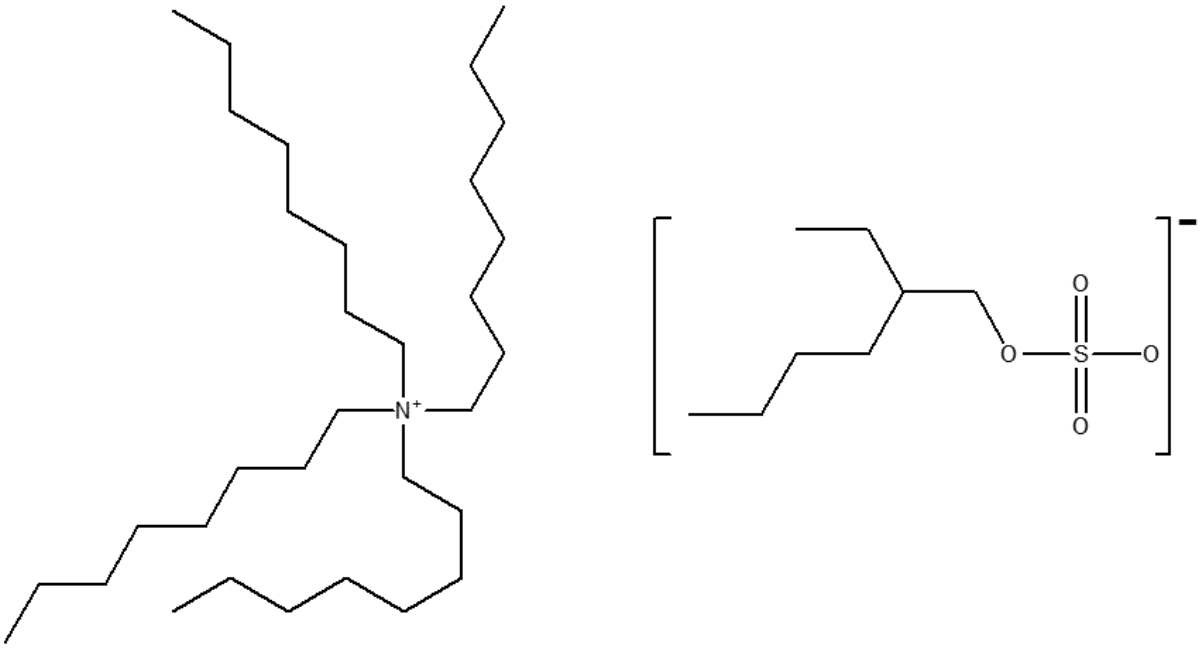

Figure S1. Chemical structures of the tetraoctylammonium cation, $[N_{8,8,8,8}]^+$, and the 2-ethylhexyl sulfate anion, $[EHS]^-$.

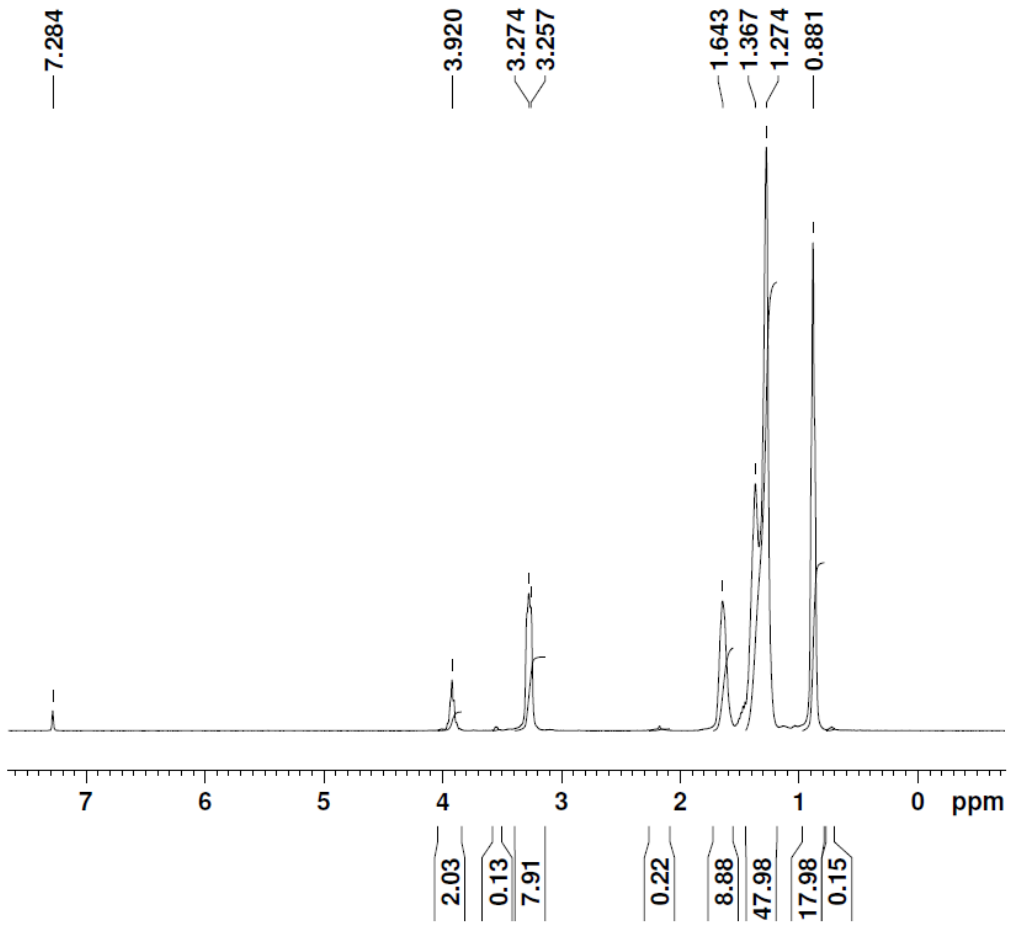

Figure S2. A ^{1}H NMR (400.212 MHz, $CDCl_3$) spectrum of $[N_{8,8,8,8}][EHS]$: 3.90-3.94 (d, 2H), 3.24-3.28 (m, 8H), 1.63-1.65 (m, 9H), 1.27-1.37 (m, 48H), 0.88 (q, 18H) ppm. A resonance line at 7.28 ppm is assigned to $CD(H)Cl_3$.

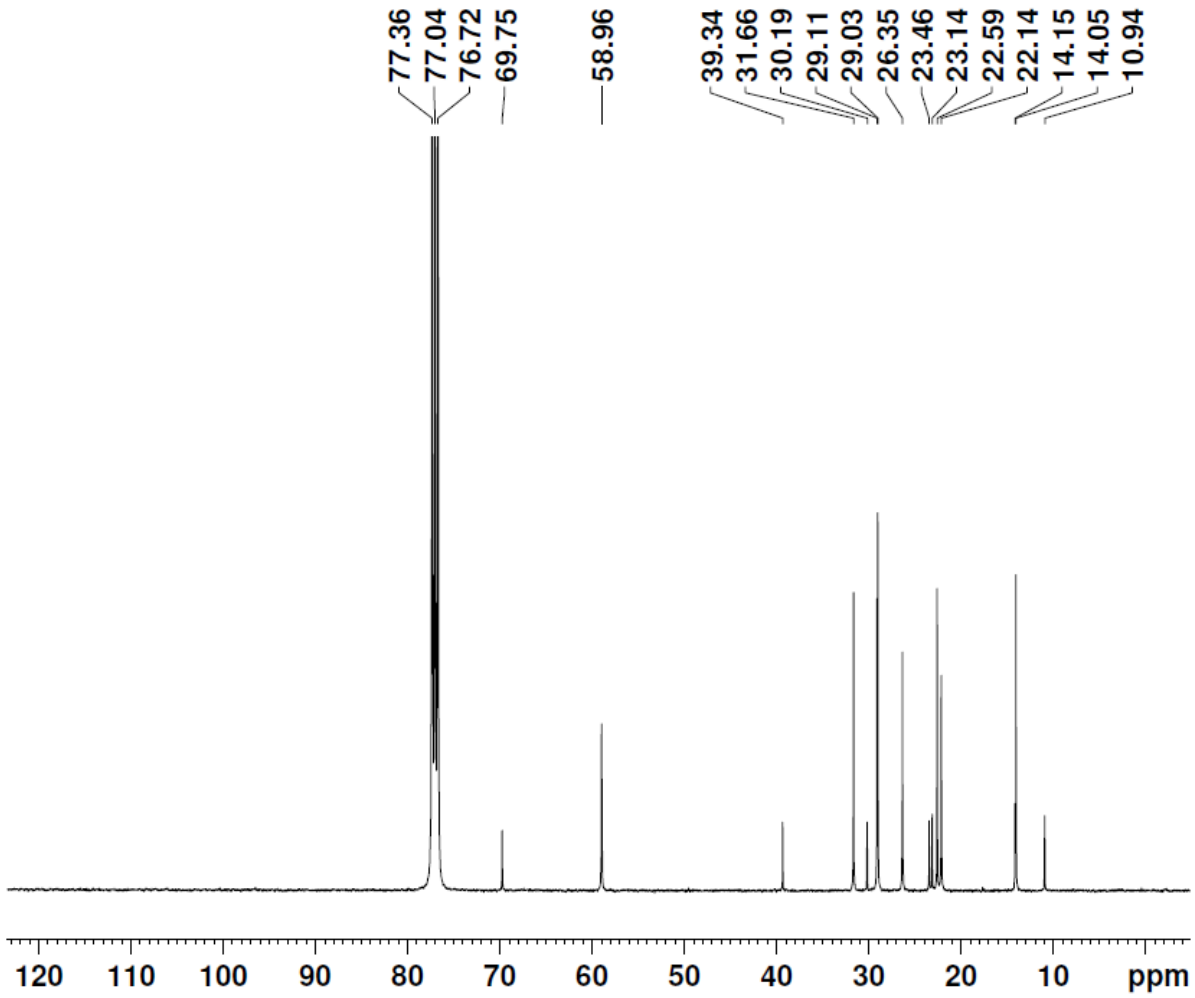

Figure S3. A ^{1}H-decoupled ^{13}C NMR (100.643 MHz, $CDCl_3$) spectrum of $[N_{8,8,8,8}][EHS]$: ^{13}C chemical shifts are assigned to aliphatic carbons in $[N_{8,8,8,8}]^+$ and $[EHS]^-$: 69.75, 58.96, 39.34, 31.66, 30.19, 29.11, 29.03, 26.35, 23.46, 23.14, 22.59, 22.14, 14.15, 14.05 and 10.94 ppm. A triplet at 77.04 ppm corresponds to the solvent, $CD(H)Cl_3$.

Table S1. Residual impurities in $[N_{8,8,8,8}][EHS]$ analyzed using an Inductive Coupled Plasma Atomic Emission Spectroscopy (ICP-AES).

Elements	Concentration (mg/kg)
Br	456
Cl	< 400
Na	< 100

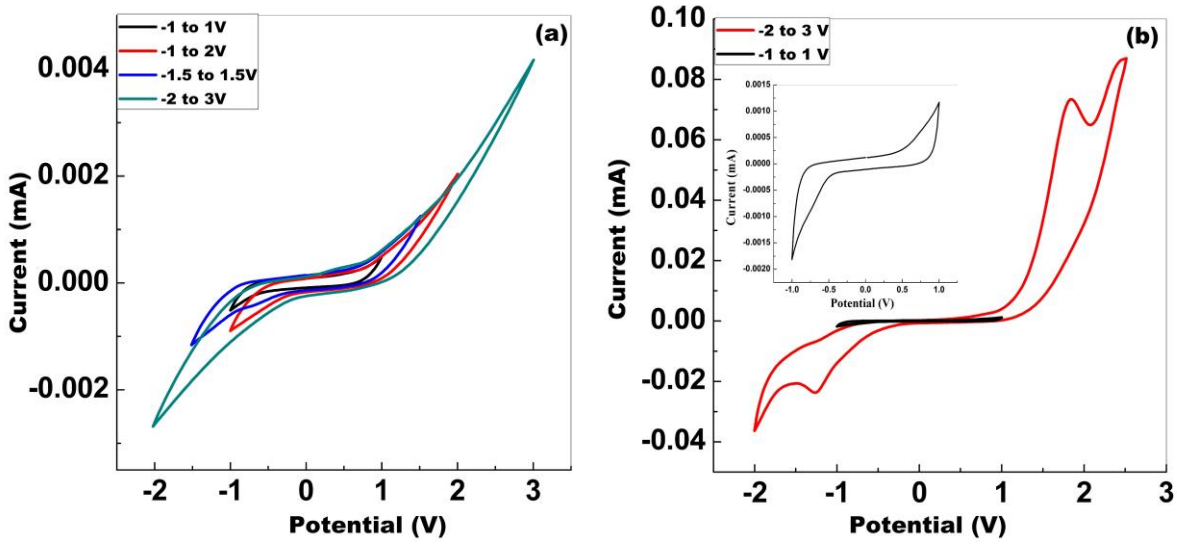

Figure S4. Electrochemical potential window on the GC electrodes for neat $[N_{8,8,8,8}][EHS]$ (**a**) and a 50 wt% binary mixture of $[N_{8,8,8,8}][EHS]$ with AcN (**b**) at 293 K. The scan rate was 100 mV s^{-1}.

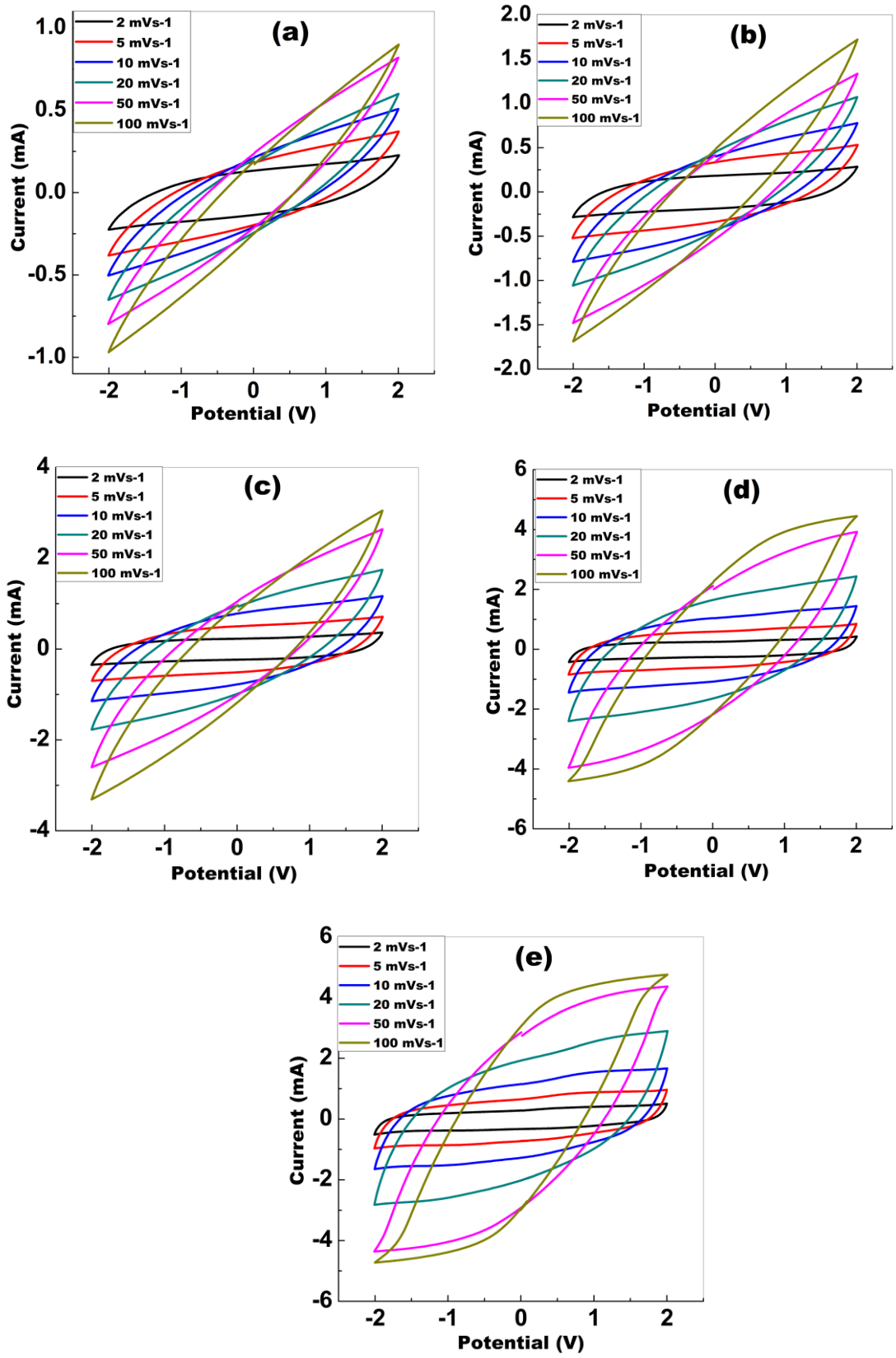

Figure S5. CV curves obtained at different scan rates for [$N_{8,8,8,8}$][EHS] as an electrolyte with MWCNTs-based electrodes in the supercapacitor cell at different temperatures 298 K (**a**), 313 K (**b**), 333 K (**c**), 353 K (**d**) and 373 K (**e**). The total weight of the electrodes is 20 mg.

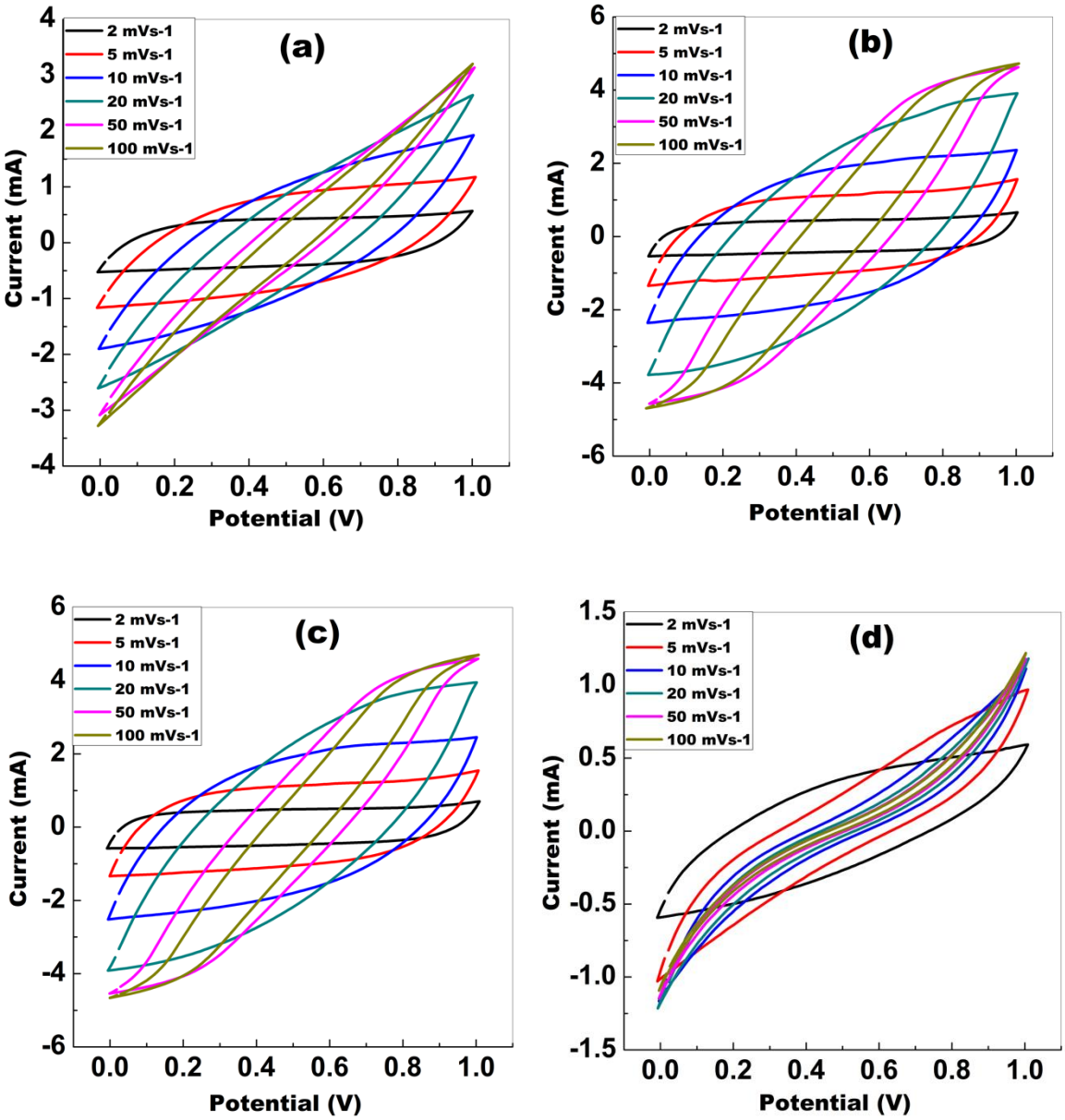

Figure S6. CV curves obtained at different scan rates for 6 M KOH(aq) as an electrolyte with MWCNTs-based electrodes in the supercapacitor cell at different temperatures 298 K (**a**), 313 K (**b**), 333 K (**c**) and 353 K (**d**). The total weight of the electrodes is 20 mg.

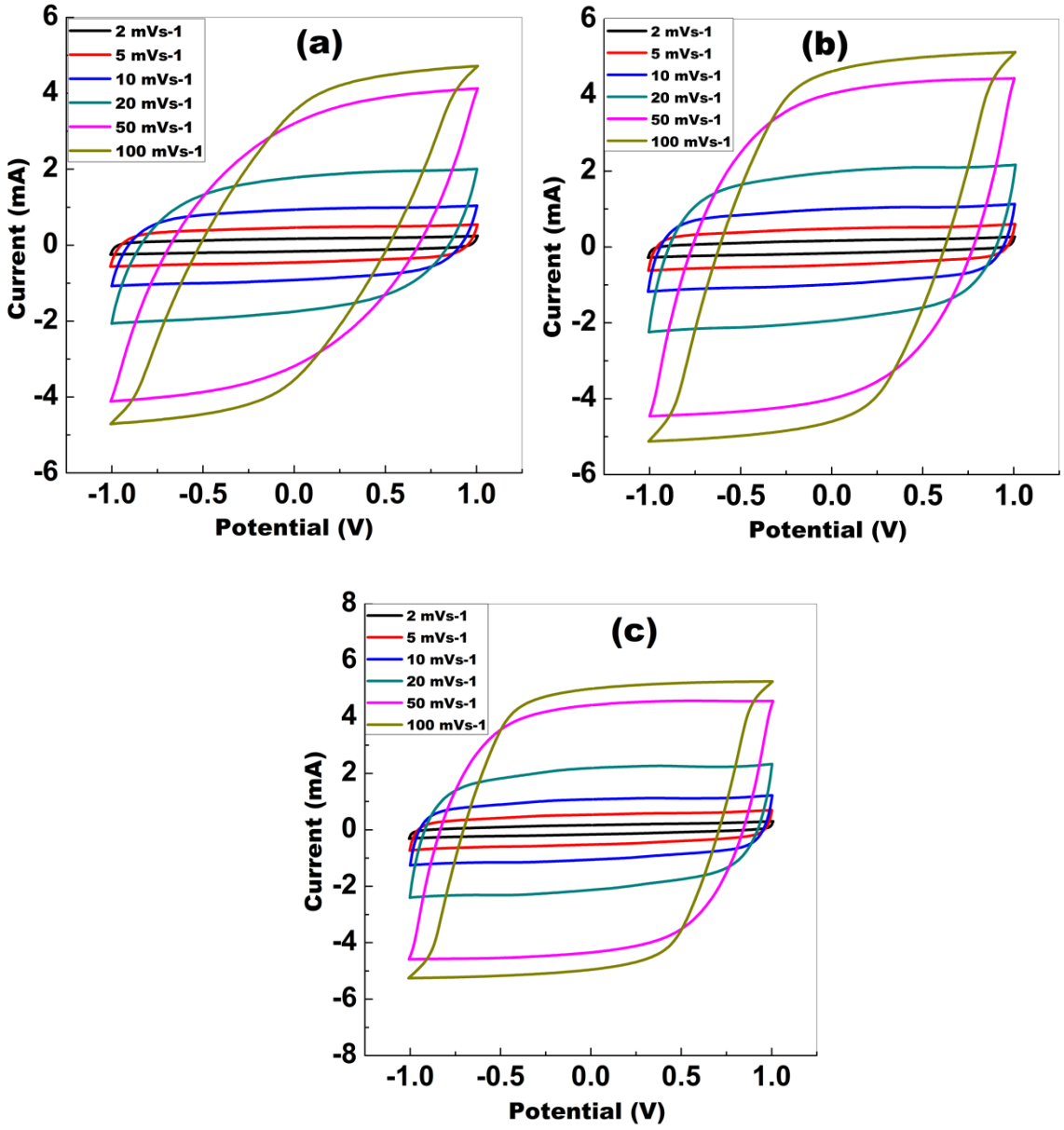

Figure S7. CV curves obtained at different scan rates for a 50 wt% mixture of $[N_{8,8,8,8}][EHS]$ with AcN as an electrolyte with MWCNTs-based electrodes in the supercapacitor cell at different temperatures 253 K (**a**), 273 K (**b**) and 298 K (**c**). The total weight of the electrodes is 20 mg.

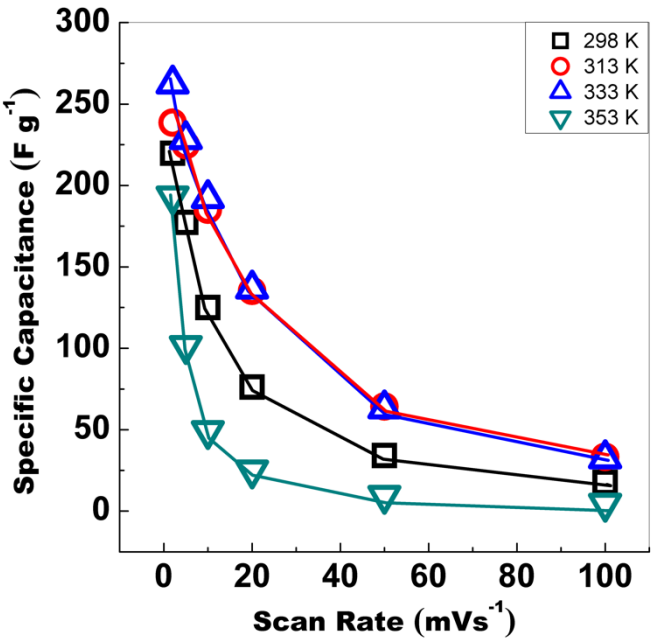

Figure S8. The specific capacitance (C_{elec}) as a function of the scan rate for 6 M KOH(aq) as an electrolyte with MWCNTs-based electrodes in the supercapacitor cell (measured at different temperatures between 298 and 353 K).

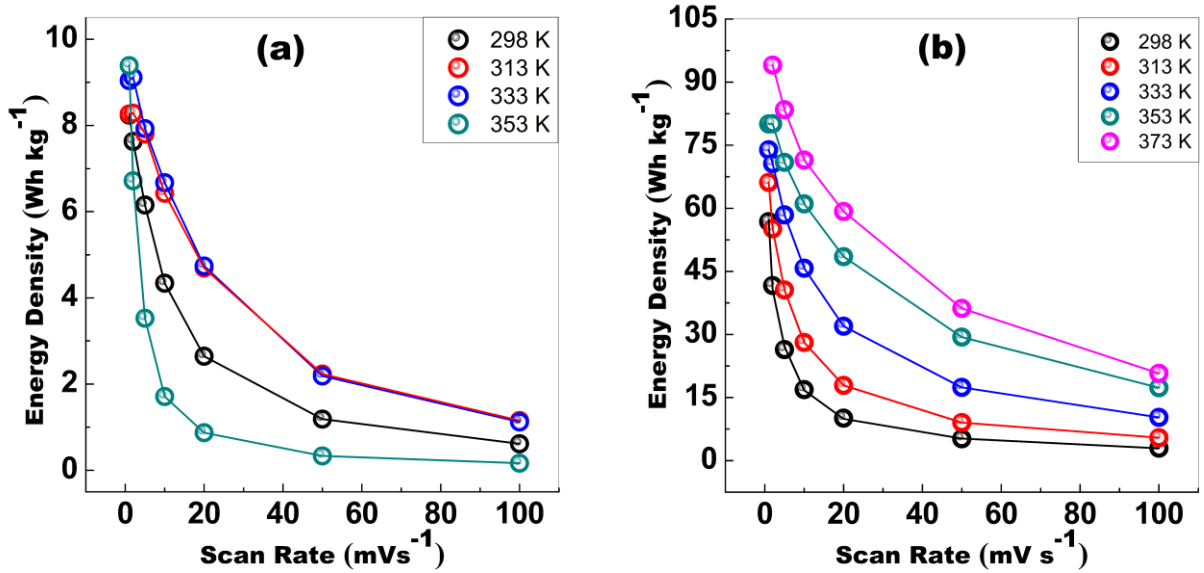

Figure S9. Energy density as a function of the scan rate for 6 M KOH(aq) (**a**) and [$N_{8,8,8,8}$][EHS] (**b**) as electrolytes with MWCNTs-based electrodes in the supercapacitor cell measured at different temperatures.

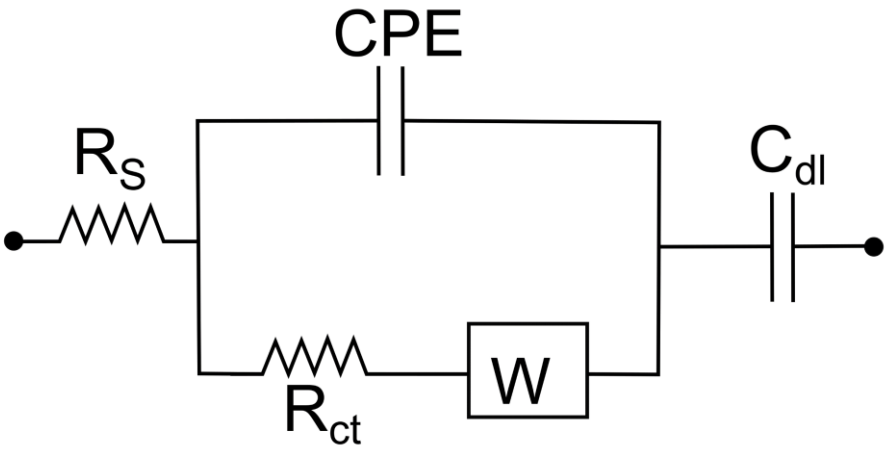

Figure S10. Modified Randal's circuit used for the fitting of EIS data. Where, R_s is the solution resistance, R_{ct} is the charge transfer resistance, *CPE* is the constant phase element, *W* is the Warburg frequency and C_{dl} is the double layer capacitance.

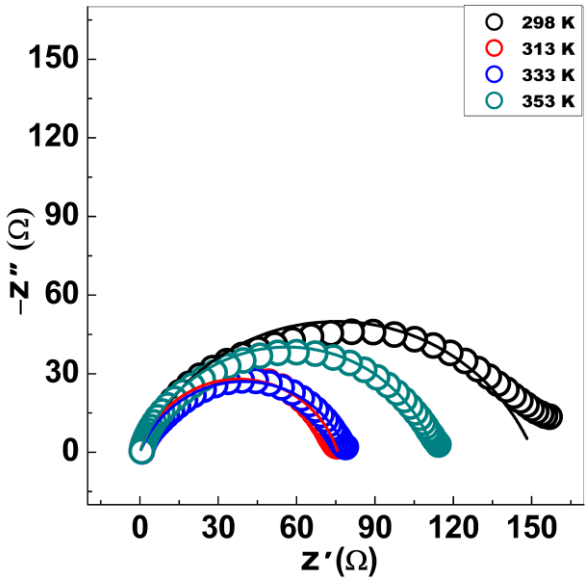

Figure S11. Nyquist plots obtained for 6 M KOH(aq) as an electrolyte with MWCNTs-based electrodes in the supercapacitor cell at different temperatures: 298 K, 313 K, 333 K and 353 K.

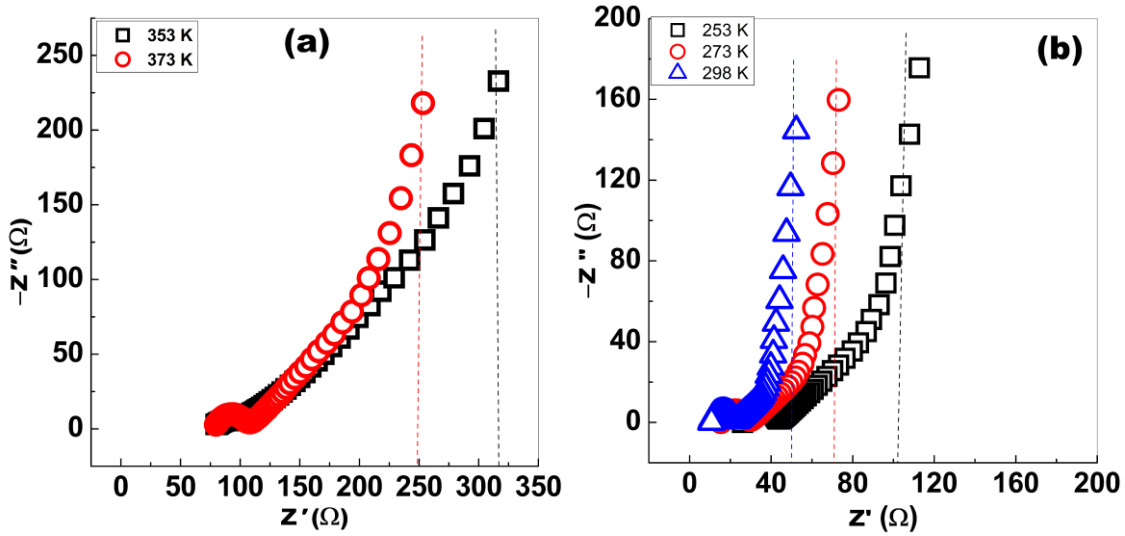

Figure S12. Nyquist plots obtained for [$N_{8,8,8,8}$][EHS] (**a**) and a 50 wt% mixture of [$N_{8,8,8,8}$][EHS] with AcN (**b**) as electrolytes with MWCNTs-based electrodes in the supercapacitor cell at different temperatures. The ESR is estimated using extrapolations (see vertical broken lines).

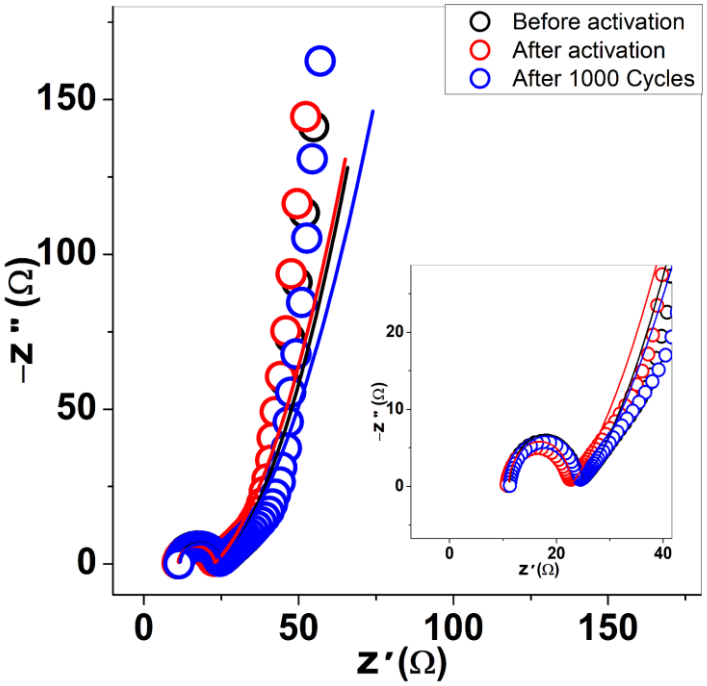

Figure S13. Nyquist plots obtained for a 50 wt% mixture of [$N_{8,8,8,8}$][EHS] with AcN as an electrolyte with MWCNTs-based electrodes in the supercapacitor cell before and after activation (50 cycles at 5 mV s^{-1} at 298 K) and after 1000 cycles at 50 mV s^{-1} at 298 K.

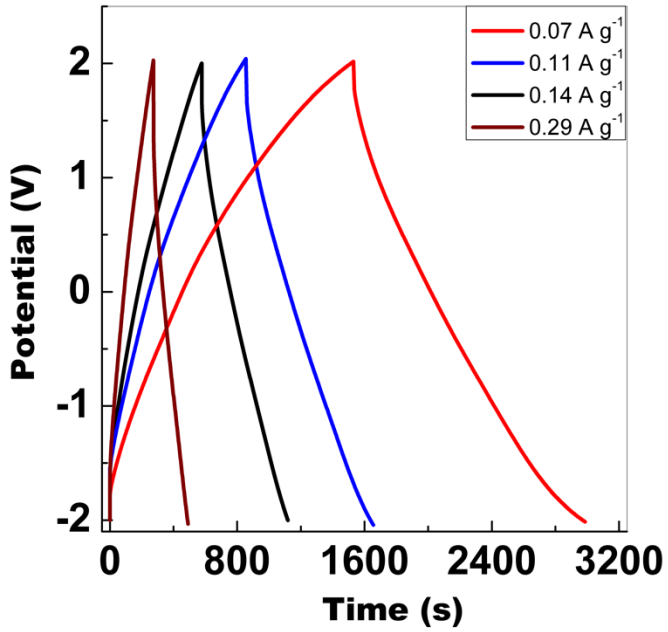

Figure S14. GCD curves at different current densities obtained for [$N_{8,8,8,8}$][EHS] as an electrolyte with MWCNTs-based electrodes in the supercapacitor cell at 373 K.

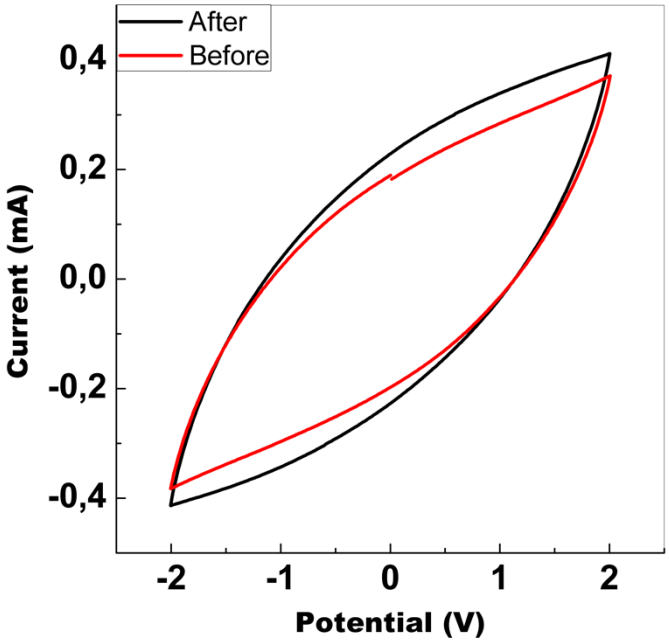

Figure S15. CV curves obtained for [$N_{8,8,8,8}$][EHS] as an electrolyte with MWCNTs-based electrodes in the supercapacitor cell at the scan rate of 5 mV s^{-1} and at 298 K, before (black curve) and after (red curve) continuous electrochemical experiments from 298 to 373 K for about 5 days (around 250 cycles in the range from 298 K to 373 K at different scan rates, EIS and GCD experiments. The time when we used this supercapacitor devices at various temperatures is almost equal when we do around 2700 CV cycles at 50 mVs^{-1}). The total weight of the electrodes is 20 mg.

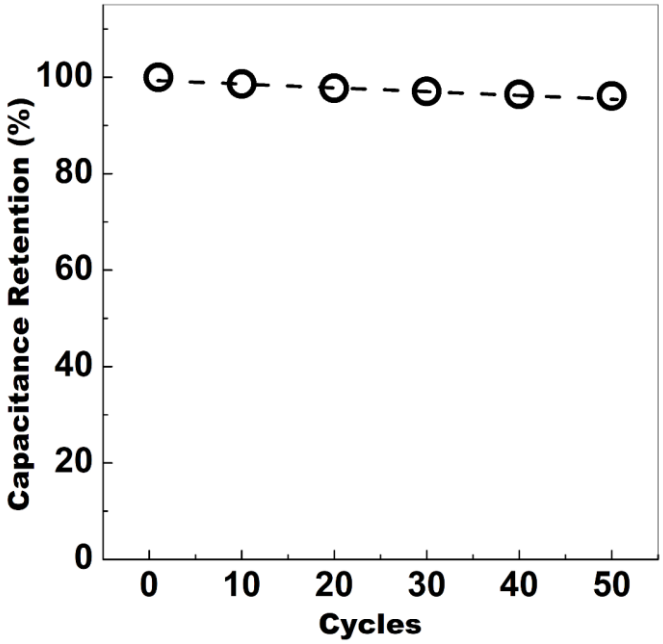

Figure S16. The capacitance retention of CV cycles (50 cycles) at 5 mV s^{-1} and 298 K after completing all the experiments from 298 to 373 K for the MWCNT-based electrode and neat SAIL as an electrolyte.

Table S2. Performance comparison of a MWCNTs-based supercapacitor with different IL-based electrolytes from literature.

Electrode Material[a]	Electrolytes[b]	Electrochemical window	Thermal Stability	E (W h kg^{-1})	References
MWCNTs	$[N_{8,8,8,8}][EHS]$ (298 K)	4V	≅527 K	41.63	This work
MWCNTs	$[N_{8,8,8,8}][EHS]$ (373 K)	4V	≅527 K	94.05	This work
MWCNTs	50:50 (wt/wt) $[N_{8,8,8,8}][EHS]$/ Acetonitrile (298 K)	2V	-	15.68	This work
MWCNTs	6M KOH (aq) (298 K)	1V	≅353 K	8.24	This work
MWCNTs	$[C_4C_1Im][AOT]$[b] (298 K)	4V	≅523 K	≅170	Ref[S1]
AC[a]	SPE-(PEO-A):IL[c] (298 K)	3V	≅553 K	41.24	Ref[S2]
AC[a]	PAEK-PEG/$LiClO_4$[d] (393 K)	1.5 V	≅385 K	6.76	Ref[S3]
AC[a]	PAES-Q-1.1[e] (298 K)	1 V	≅558 K	2.61	Ref[S4]
Hybrid Carbon	$[P_{4,4,4,4}][FuA]$[f] (293 K)	3.2 V	≅564 K	29.00	Ref[S5]

[a]AC in this table represents activated carbon;

[b]$[C_4C_1Im][AOT]$ = 1-butyl-3-methylimidazolium 1,4-bis(2-ethylhexoxy)-1,4-dioxobutane-2-sulfonate;

[c]SPE-(PEO-A):IL = solid polymer electrolyte-poly(ethylene oxide)-co-poly(propylene oxide) copolymer cross-linked by a bisphenol-A diglycidyl ether in 1-ethyl-3-methylimidazolium bis(trifluoromethylsulfonyl)imide (i.e., EMImTFSI);

[d]PAEK-PEG/LiClO4 = poly(aryl ether ketone)–poly(ethylene glycol) copolymer as a polymer host and $LiClO_4$ as an electrolyte salt;

[e]PAES-Q-1.1 separator is prepared by quaternary ammonium functionalized poly(arylene ether sulfone) copolymer;

[f]$[P_{4,4,4,4}][FuA]$: = tetra(*n*-butyl)phosphonium furoate.

References:

1. Mao, X.; Brown, P.; Cervinka, C.; Hazell, G.; Li, H.; Ren, Y.; Chen, D.; Atkin, R.; Eastoe, J.; Grillo, I.; Padua, A. A. H.; Costa Gomes, M. F.; Hatton, T. A., Self-assembled nanostructures in ionic liquids facilitate charge storage at electrified interfaces. *Nat. Mater.* **2019,** *18* (12), 1350-1357.

2. Na, R. Q.; Su, C. W.; Su, Y. H.; Chen, Y. C.; Chen, Y. M.; Wang, G. B.; Teng, H. S., Solvent-free synthesis of an ionic liquid integrated ether-abundant polymer as a solid electrolyte for flexible electric double-layer capacitors. *J. Mat. Chem. A* **2017,** *5* (37), 19703-19713.

3. Na, R.; Huo, P.; Zhang, X.; Zhang, S.; Du, Y.; Zhu, K.; Lu, Y.; Zhang, M.; Luan, J.; Wang, G., A flexible solid-state supercapacitor based on a poly(aryl ether ketone)–poly(ethylene

glycol) copolymer solid polymer electrolyte for high temperature applications. *RSC Advances* **2016,** *6* (69), 65186-65195.

4. Huo, P. F.; Zhang, S. L.; Zhang, X. R.; Geng, Z.; Luan, J. S.; Wang, G. B., Quaternary ammonium functionalized poly(aryl ether sulfone)s as separators for supercapacitors based on activated carbon electrodes. *J. Membr. Sci.* **2015,** *475*, 562-570.

5. Khan, I. A.; Shah, F. U., Fluorine-free ionic liquid-based electrolyte for supercapacitors operating at elevated temperatures. *ACS Sust. Chem. Eng.* **2020,** *8* (27), 10212-10221.